Implicit and Explicit Solvent Models for the Simulation of Dilute Polymer Solutions

Govardhan Reddy and Arun Yethiraj*

Theoretical Chemistry Institute and Department of Chemistry, University of Wisconsin, Madison, Wisconsin 53706

Received May 25, 2006; Revised Manuscript Received September 21, 2006

ABSTRACT: Computer simulations of dilute polymer solutions are presented with different models for the solvent. Three different problems are studied: the collapse dynamics of a neutral polymer chain, the conformational properties of a polyelectrolyte chain in a poor solvent, and the adsorption of a polyelectrolyte chain near a charged planar surface. In addition to an explicit solvent model where the solvent atoms are incorporated as a second component, two implicit solvent models are also studied. In the first, called implicit Lennard-Jones (ILJ), the effect of solvent is taken into account via a Lennard-Jones pair potential between the monomers, and in the second, called SASA, the solvent is taken into account via a many-body interaction that depends on the solvent-accessible surface area (SASA) of the monomers. In all cases, there are qualitative differences between the properties predicted by the ILJ and the explicit solvent model. In particular, the ILJ predicts the trapping of a collapsing neutral polymer in metastable states, stable bead−necklace structures of polyelectrolytes in poor solvents, and globule formation without adsorption for polyelectrolytes in poor solvents at a charged surface. For similar systems, on the other hand, the explicit solvent model predicts a smooth collapse, transient bead−necklace structures, and adsorption flat against the surface, respectively. The predictions of the SASA model are in qualitative agreement with the explicit solvent simulations in all cases, although there are quantitative differences. This emphasizes the importance of many-body solvent effects and suggests a computationally tractable way of incorporating them.

I. Introduction

The static and dynamic properties of dilute polymer solutions depend strongly on the nature and quality of the solvent, and the properties of polymers, especially charged polymers, in poor solvents is a topic of current interest. In the case of polyelectrolytes, ionizable groups are substituted along the otherwise hydrophobic polymer molecule in order to make them water-soluble. The result is a strong solvent-induced effective interaction between two polymer beads which is balanced by the electrostatic repulsion between charged moieties. This competition results in interesting conformational properties that have been widely studied.

Computer simulations have played a very important role in our understanding of the properties of polymers[1−7] and proteins in solution.[8−10] Simulations are particularly useful for dilute solutions where experimental scattering techniques are challenging because of low intensity. In principle, one can create an initial configuration with polymer and solvent and propagate the system using standard techniques, e.g., molecular dynamics. In dilute solutions, however, the solvent molecules are an enormous inconvenience because the majority of the system is composed of solvent molecules whose properties are of little interest. Implicit solvent models, where the solvent is replaced by an effective interaction between the polymer beads, are therefore of considerable importance, given the potentially significant savings in computational time. This is particularly true in polymer solutions where the time scales of interest are large compared to that of the solvent dynamics.

A particularly simple implicit solvent model is one where the solvent is replaced by an effective pairwise attraction between the polymer beads. There are many studies in the literature[11] of the implicit Lennard-Jones (ILJ) model where the solvent is replaced by a pairwise additive Lennard-Jones (LJ) interaction between polymer beads. A decrease in solvent quality corresponds to an increase in the well depth in the LJ interaction. This model is qualitatively correct for the static properties in the sense that it causes the polymer to collapse as the solvent quality is decreased. The well depth can always be adjusted so that the model reproduces the average conformational properties of single polymer chains in poor solvents.

The ILJ model has been shown, however, to be in qualitative error for the *dynamic* and *thermodynamic* properties of polymers in poor solvents. In a series of papers, Chang and Yethiraj[12,13] studied the effect of solvent on the properties of neutral and charged polymers. They compared molecular dynamics (MD) with explicit solvent to Brownian dynamics (BD) simulations with ILJ solvent and showed that the predictions of these two models were qualitatively different in many cases. For the collapse dynamics of a neutral homopolymer, they showed that the explicit solvent model showed a rapid collapse under all conditions whereas in the ILJ solvent model the polymer was trapped in local minima. For polyelectrolyte solutions, explicit solvent simulations showed phase separation while ILJ simulations suggested the formation of gel-like structures. They attributed these differences to the fact that solvent-induced effects are patently not pairwise decomposable. In the ILJ model, two polymer sites on the interior of a collapsed structure feel a very strong attractive interaction while in reality the interaction is just the weak dispersion interaction between monomers. For polyelectrolytes, the difference could be more dramatic because the bead−bead interactions can be attractive with the ILJ solvent and repulsive with an explicit solvent, thus leading to qualitatively different physics. Although instructive, these simulations do not solve the problem because explicit solvent simulations are prohibitively intensive for large polymers.

In this work, we investigate the properties of polymer solutions using a simple many-body solvent model borrowed

* Corresponding author. E-mail: yethiraj@chem.wisc.edu.

10.1021/ma061176+ CCC: $33.50
Published on Web 10/28/2006

from biophysics. Sophisticated implicit solvent models[14] are used in the simulation of biological macromolecules, but these techniques are not yet popular in the simulation of polymeric systems. The simplest many-body solvent model is one where the solvent-induced interaction depends on the solvent-accessible surface area (SASA) of the macromolecule. This incorporates the primary effect discussed by Chang and Yethiraj,[12,15] i.e., that the solvent interaction is a surface effect rather than a pairwise additive effect. Several approximate schemes to efficiently calculate the SASA have been proposed. In this paper, we test one such scheme[16] and compare the predictions of this implicit solvent model, which we refer to as SASA, to explicit solvent and ILJ simulations. We find that the predictions of SASA are qualitatively similar to those of the explicit solvent for three different problems: the collapse dynamics of homopolymers, the conformational properties of single charged chains, and the adsorption of charged chains to a surface. The SASA is therefore a promising candidate for simulations of dilute polymer solutions.

The rest of the paper is organized as follows. In section II we describe the models and simulation method, in section III present and discuss the results, and in section IV present some conclusions.

II. Molecular Model and Simulation Method

A. Bonding and Electrostatic Interactions. In all cases, the polymer molecules are modeled as flexible bead−spring chains. The bonding potential between neighboring monomers along the backbone is given by the FENE (finite extensible nonlinear elastic) potential[17]

$$V_{\mathrm{FENE}}(r) = -\frac{1}{2}k_{\mathrm{FENE}}{R_0}^2 \ln\left(1 - \frac{r^2}{{R_0}^2}\right) \tag{1}$$

where k_B is Boltzmann's constant, T is the temperature, k_{FENE} is the spring constant, and R_0 is the maximum extension of the bond. In this work, we set $k_{\mathrm{FENE}} = 30.0k_BT/\sigma^2$ and $R_0 = 1.5\sigma$; these parameters prevent[17] the crossing of the chains. The parameter σ is used as the unit of length in this work and is the collision diameter of the Lennard-Jones (LJ) potential

$$V_{\mathrm{LJ}}(r) = 4\epsilon_{\mathrm{LJ}}\left[\left(\frac{\sigma}{r}\right)^{12} - \left(\frac{\sigma}{r}\right)^{6}\right] \tag{2}$$

The total potential of interaction between any two sites is the sum of a nonelectrostatic and electrostatic interaction. The monomers interact via a site−site nonelectrostatic interaction potential that is different for the different solvent models. If the polymer is charged, each monomer carries a unit negative charge, and an equal number of positively charge counterions, of the same size as the monomers, are added to balance this charge. The electrostatic interaction, $V_{ij}^{\mathrm{el}}(r)$, is given by

$$V_{ij}^{\mathrm{el}}(r) = k_BT\frac{q_iq_j\lambda_B}{r} \tag{3}$$

where q_i is the charge valence of the site i, $\lambda_B \equiv e^2/\epsilon k_BT$ is the Bjerrum length, e is the unit charge, and ϵ is the dielectric constant of the solvent. This interaction is taken to be the same in *all* the solvent models; i.e., the nature of the solvent does not alter the electrostatic interactions between ions.

For the simulation of polyion adsorption on charged surfaces, two surfaces are added along the z direction of the simulation box. The nonelectrostatic interaction between the particles and the surface is purely repulsive and is given by[18]

$$V_{\mathrm{wall}} = \begin{cases} 2\pi\epsilon_w{\sigma_w}^2\left[\frac{2}{5}\left(\frac{\sigma_w}{z}\right)^{10} - \left(\frac{\sigma_w}{z}\right)^4 + \frac{3}{5}\right] & z \le \sigma_w \\ 0 & z > \sigma_w \end{cases} \tag{4}$$

where z is the perpendicular distance from the particle to the solid surface and the subscript w denotes the surface. This potential is obtained from the integration of the 12−6 LJ potential of a planar solid continuum in the two directions parallel to the surface. We set $\epsilon_w = \epsilon_{\mathrm{LJ}}$ and $\sigma_w = \sigma$ for all the particles present in the simulation box. Both the surfaces interact with the particles in the simulation cell using the soft core repulsive LJ potential given by eq 4, but only one of the surfaces is electrically charged. The co-ions, which have a charge opposite in sign to that of the surface, balance the charge on the surface. The electric field, E_j, acting on a charged particle j due to the uniform charge density, σ_{SCD}, on a nonconducting surface is given by $E_j = \sigma_{\mathrm{SCD}}/2\epsilon$, and the direction of E_j is perpendicular to the surface.

B. Explicit Solvent Model. In this model, the solvent molecules are incorporated explicitly as an additional component. The nonelectrostatic interaction, V_{ij}^{st}, between sites i and j is given by

$$V_{ij}^{\mathrm{st}}(r) = \lambda_{ij}V_{\mathrm{CLJ}}(r) + (1 - \lambda_{ij})V_{\mathrm{WCA}}(r) \tag{5}$$

where $V_{\mathrm{CLJ}}(r)$ is the cut and shifted LJ and $V_{\mathrm{WCA}}(r)$ is a purely repulsive LJ potential;[19] i.e., $V_{\mathrm{CLJ}}(r)$ is obtained by truncating $V_{\mathrm{LJ}}(r)$ at $r = 2.5\sigma$ and shifting it so that $V_{\mathrm{CLJ}}(2.5\sigma) = 0$, and $V_{\mathrm{WCA}}(r)$ is obtained by truncating $V_{\mathrm{LJ}}(r)$ at $r = 2^{1/6}\sigma$ and shifting it so that $V_{\mathrm{WCA}}(2^{1/6}\sigma) = 0$.

The solvent quality is determined via the λ_{ij} parameters. Following previous work,[15] we set $\lambda_{ij} = \lambda$ between any two solvent molecules or any two monomers, and $\lambda_{ij} = 0$ otherwise. Note that the nonelectrostatic contribution to the potential is purely repulsive for all pairs of sites except for the monomer−monomer and solvent−solvent pairs, where it is attractive for $\lambda > 0$. When $\lambda = 0$, all nonelectrostatic interactions are identical and therefore the solvent quality is good. On the other hand, when $\lambda = 1$, there are attractions between monomers and between solvent molecules but the monomer−solvent interaction is purely repulsive, and this makes the solvent quality poor.

C. Implicit Lennard-Jones (ILJ) Model. The ILJ model is the crudest, but most popular, model for the solvent. In this model, the solvent is not incorporated explicitly, and the effective nonelectrostatic interaction between polymer sites is given by

$$V^{\mathrm{st}}(r) = V_{\mathrm{WCA}}(r) + V_{\mathrm{CLJ}}(r) \tag{6}$$

where $V_{\mathrm{WCA}}(r)$ and $V_{\mathrm{CLJ}}(r)$ are the repulsive and attractive LJ potentials described in the previous section. As ϵ_{LJ} is increased, the strength of the interaction between the polymer beads increases, and therefore the solvent quality decreases. We define a reduced quantity $\epsilon_{\mathrm{LJ}}^* \equiv \epsilon_{\mathrm{LJ}}/k_BT$.

D. Solvent-Accessible Surface Area (SASA) Model. In the SASA model the potential on a monomer due to the solvent is evaluated using the amount of surface area of the monomer exposed to the solvent. The effective nonelectrostatic interaction between polymer sites is given by

$$V^{\mathrm{st}}(r) = V_{\mathrm{WCA}}(r) + V_{\mathrm{sol}}(r) \tag{7}$$

The solvation free energy, $V_{\mathrm{sol}}(r)$, is assumed to be the sum of

the contributions from all the monomers, i.e.

$$V_{sol}(r) = \sum_{i=1}^{N} g_i \gamma_i \tag{8}$$

Here the summation is over all the monomers, and g_i is the solvation energy per unit area for the monomer i. Since all the monomers are identical in a polymer, we assume, $g_i = g$. γ_i is the accessible surface area of the monomer i exposed to the solvent, defined[16] as the area of the surface over which a solvent molecule can be placed while making van der Waals contact with the monomer and not penetrating any other monomer or atom. The solvent-accessible surface area of the monomers and the forces arising from the solvation potential are calculated using the method of Wodak and Janin[16] using a probe radius of $\sigma/2$ for the solvent molecule. We define a reduced quantity $g^* \equiv g\sigma^2/k_B$. In polyelectrolyte simulations, counterions and co-ions are ignored in the calculation of the surface area of the polyelectrolyte exposed to the solvent. This makes the quality of the ions poor to the polymer backbone as the solvent quality is decreased, and this assumption is qualitatively present in all three simulation models.

E. Simulation Method. In the explicit solvent simulations, the polymer molecule, counterions, and co-ions (if any) are first inserted into the simulation cell, and the solvent atoms are then added so that the total number density of the simulation box, $\rho_{tot}\sigma^3 = 0.864$. Periodic boundary conditions are applied in all the three directions, except for the cases where the fluid is confined between surfaces, in which case periodic boundary conditions are applied only in the other two directions. Lengths are measured in units of σ, time in units of $\tau_{MD} = (m\sigma^2/\epsilon_{LJ})^{1/2}$, and temperature in units of ϵ_{LJ}/k_B. In this calculation, we set all the three parameters m, σ, and ϵ_{LJ} to unity and define a reduced temperature as $T^* \equiv k_BT/\epsilon_{LJ}$, which is set equal to 1. Initial velocities are generated using a Gaussian random number generator and scaled to the desired temperature. The system is propagated in the canonical ensemble (*NVT* constant) using a explicit reversible integrator[20] with temperature maintained constant using a Nose−Hoover thermostat.[21,22] An integration time step of $0.005\tau_{MD}$ is used, and the Nose−Hoover coupling constant is set to 5. Further simulation details can be found elsewhere.[13]

The Brownian dynamics simulation algorithm used for the implicit solvent models is a straightforward implementation of the Ermak and McCammon[23] algorithm without hydrodynamic interactions. Time is measured in units of σ^2/D_0, where D_0 is the monomeric diffusion constant. We define $\tau_{BD} \equiv \sigma^2/D_0$. An integration time step of $0.0001\tau_{BD}$ is used and the simulation is equilibrated for 2−5 million time steps before averages are calculated.

III. Results and Discussion

The solvent quality gets poorer (in the various models) as the parameters λ (explicit solvent), ϵ^* (ILJ), and g^* (SASA) are increased. Although we are primarily interested in qualitative differences between these models, it is important to be able to map the parameters of each model onto the others. To calibrate the solvent quality in these models, we compare the radius of gyration of a $N = 16$ bead neutral chain for the three different models as a function of their respective solvent quality parameters in Figure 1. As expected, when the solvent quality is decreased, the chain collapses. From a plot such as this (for $N = 16$), we map $\lambda = 0.2$ (for $\epsilon_{LJ} = 1$) to $g^* = 0.5$ and $\epsilon^* = 1$. This mapping is a strong function of the chain length, but a similar procedure is used in all cases studied; i.e., when two models are compared, the solvent parameters of the models are chosen so that the equilibrium size of the *neutral* chain is the same (within statistical uncertainties) in both the models. Although the chains can be trapped in metastable states when the solvent quality is decreased suddenly, this does not happen when the solvent quality is decreased in small steps followed by equilibration at each stage, which is how the results in Figure 1 are obtained.

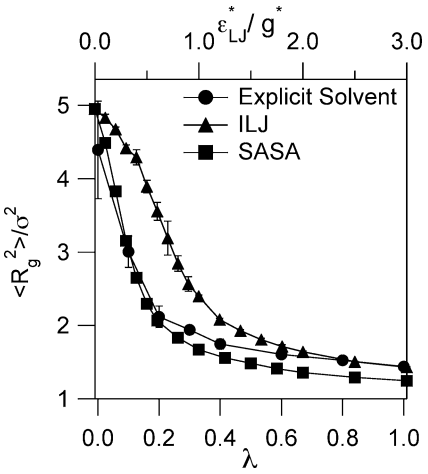

Figure 1. Variation of the mean-square radius of gyration with solvent quality parameters for various models, for $N = 16$. Bottom and top scales show the quenching depths for explicit and implicit solvent models, respectively.

A. Collapse Dynamics of a Neutral Polymer Chain. In good solvents, a polymer chain takes on an expanded self-avoiding random walk conformation. When the solvent quality is sufficiently poor, the conformation is that of a collapsed spherical globule. The dynamics of the collapse of the chain when the solvent quality is suddenly changed, e.g., by quenching to a low temperature, is of interest. Previous simulations[12,24−36] present a consistent picture of the sequence of events. Localized blobs of monomers separated by linear chains are first formed. These blobs grow in size at the expense of the linear chains and then coalesce into a sausage-like conformation. The beads in the sausage-like conformation then reorganize to create a spherical globule.

Chang and Yethiraj[12] showed that the dynamics of the collapse, however, are very different with explicit and ILJ models. With the ILJ model, the change in polymer size occurred in discrete jumps, and for deep quenches the polymer was often trapped in metastable states, especially in the sausage-like structure. For sufficiently deep quenches, the chain never reached the equilibrium state in the ILJ model. With explicit solvent, however, the chain always collapsed smoothly to the final state. In fact, the deeper the quench the more rapid was the collapse.

We find that the predictions of the SASA model are similar to that of the explicit solvent model, but the predictions of the ILJ model are distinctly different. Figure 2a,b depicts the size of a chain (degree of polymerization $N = 64$) as a function of time for various trajectories using the ILJ and SASA models. The initial conditions and quench depth are chosen so that the average initial and final radius of gyration are the same in both models. In the ILJ model (Figure 2a), there are sudden drops in the chain size while in the SASA model (Figure 2b) the decrease in chain size is continuous for all trajectories. Furthermore, in the ILJ model the chain is trapped in metastable states, often for long durations, while in the SASA model the

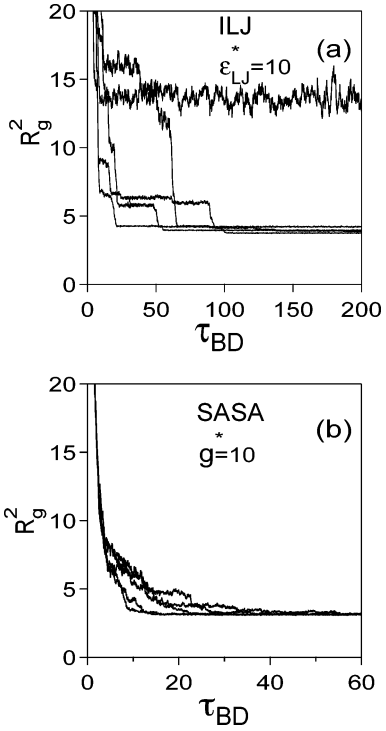

Figure 2. Independent trajectories for the variation of the square radius of gyration with time for (a) the ILJ and (b) the SASA models, for $N = 64$.

equilibrium state is reached smoothly and quickly. The predictions of the explicit solvent model are similar to the SASA model, and these are therefore not shown. A previous simulation study[34] using implicit solvent model based on the idea that solvent-induced interaction between the monomers depends on the local density of the solvent near the monomers also gave results similar to the explicit solvent and SASA simulations.

B. Equilibrium Shape of a Charged Polymer Chain. Chang and Yethiraj[15] reported explicit solvent simulations for the shape of a single polyelectrolyte chain in poor solvents. The main conclusion of this study[15] was that the pearl-necklace structure predicted by theory[37] and seen in implicit solvent simulations[38−41] is not very stable when the solvent is incorporated explicitly, and snapshots therefore did not show clear signatures of these conformations. On the basis of a cluster analysis, however, they concluded that pearl-necklace structures are consistent with their data but only loosely held together by weak forces. Here, we qualitatively compare the predictions of the SASA model for a polyelectrolyte chain in poor solvent with the explicit solvent simulation.[15]

Figure 3 compares the $\langle R_g^2 \rangle$ divided by the degree of polymerization, N, for an isolated polyelectrolyte as a function of the solvent quality, g^*, for different chain lengths. The collapse transition from an extended conformation to a collapsed globule moves to higher values of g^* with an increase in chain length, N, and also the collapse transition becomes broader as N increases. Similar behavior is seen with the ILJ model but not in explicit solvent simulations,[15] where the λ value at which the collapse transition occurs is independent of the chain length.

The SASA predictions for chain conformations are consistent with the explicit solvent simulations.[15] Figure 4 (I) depicts snapshots of configurations from the SASA model for $N = 64$, fraction of charged monomers $f = 1$, $\rho_m = 6 \times 10^{-5}$, and various values of g^*. All the monomers carry a unit charge. These conditions correspond to those for which explicit solvent simulations are available. In some cases, e.g., $g^* = 1.5$, pearl-

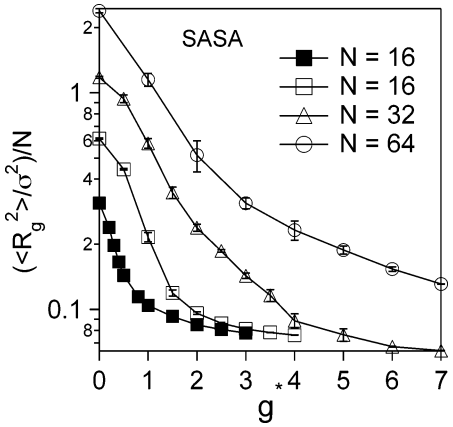

Figure 3. SASA model: $\langle R_g^2 \rangle$ as a function of g^* for various values of N. Open symbols are charged chains, and the filled symbol is an uncharged chain. The fraction of charged monomers $f = 1$ for all the chains.

like structures are observed, but these are not stable for long periods of time. As the solvent quality is decreased further, the polyelectrolyte shows structures similar to cylindrical globules. Figure 4 (II) shows snapshots for a longer chain, $N = 382$ and $f = 1/3$. Stable pearl-necklace-like structures are not observed for this chain length. As the solvent quality is decreased, the chain assumes the shape of a cylindrical globule, and the length of the globule decreases and the width increases as the solvent quality is decreased. For solvent quality $g^* = 5.5$, Figure 4 (IId) and $g^* = 6.5$ (not shown), a stable dumbbell-like structure is seen. This picture of the polyelectrolyte collapse transition is different from what is seen using the ILJ model.

Figure 5 depicts snapshots from ILJ simulations. The ILJ model predicts a strong stabilization of the pearl-necklace structures due to the strong pair attraction among the monomers inside the pearls (where there is no solvent). The dumbbell-shaped structures shown in Figure 5 are very stable, and similar looking structures are seen at the end of all the simulation runs with ILJ model. In the explicit solvent simulations[15] and the SASA model, the pearls are held together by weak surface tension forces, and these clusters are therefore not stable.

The absence of pearl-necklace conformations in the SASA model is interesting, and we perform some tests to investigate this further. Starting with a spherical conformation of a collapsed neutral chain, we gradually add charge to the beads and observe the change in the equilibrium shape. In all cases, the chain takes on cylindrical globule conformations similar to Figure 4 (II). Starting from the same initial conformation as above, if we remove the bonding potential, i.e., simulate a collection of unconnected monomers, then adding charge to the monomers results in the formation of several small spherical globules. The cylindrical globule conformation is therefore a direct consequence of bonding in the SASA model.

C. Adsorption of a Charged Polymer onto a Charged Surface. In poor solvents, the adsorption of a single polyelectrolyte chain to a charged surface is sensitive to the solvent quality.[42] Simulations presented in this paper show that for weakly charged surfaces the ILJ model predicts that the chain is a collapsed globule, but the explicit solvent model predicts that the chain adsorbs flat against the surface.[42] The SASA model is in qualitative agreement with the explicit solvent model.

The shape and orientation of the polymer can be quantified via the component of the mean-square radius of gyration

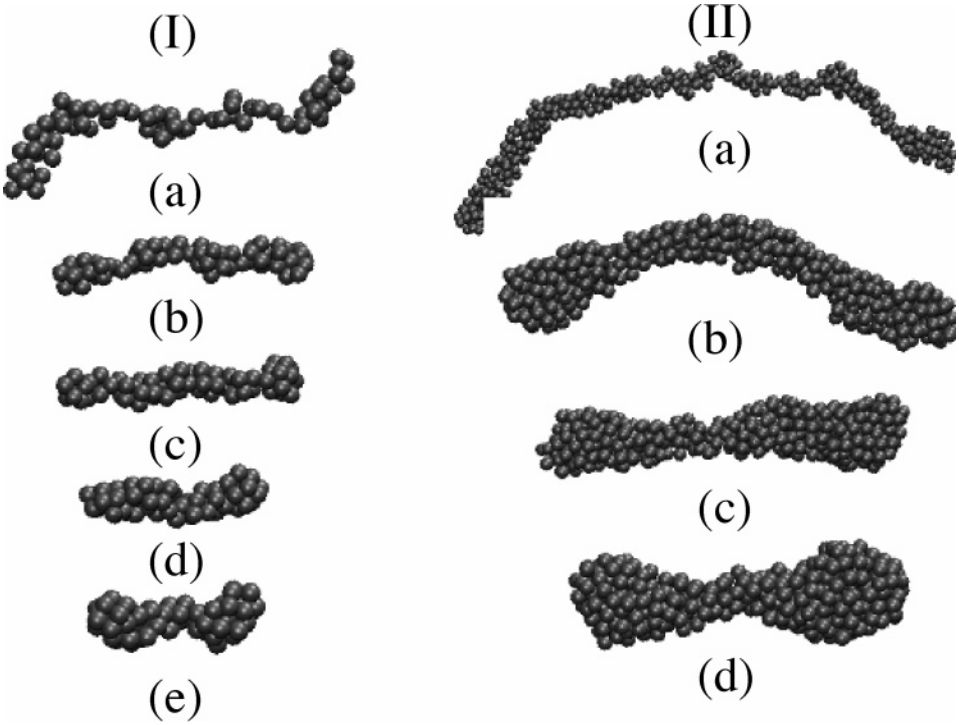

Figure 4. SASA model: (I) $N = 64$, $f = 1$, $g^* =$ (a) 1.5, (b) 2.0, (c) 2.5, (d) 4.0, and (e) 5.0; (II) $N = 382$, $f = 1/3$, $g^* =$ (a) 1.5, (b) 3.5, (c) 4.5, and (d) 5.5.

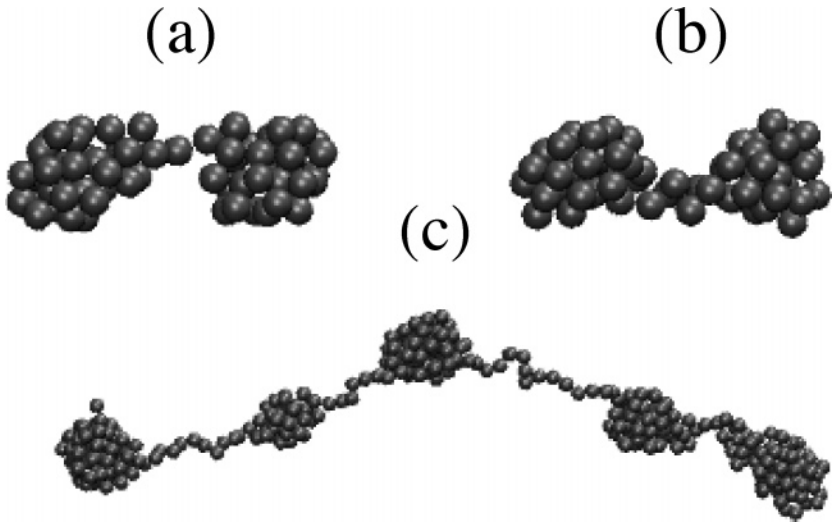

Figure 5. ILJ model: (a) $N = 64$, $f = 1$, $\epsilon^*_{LJ} = 3.5$; (b) $N = 64$, $f = 1$, $\epsilon^*_{LJ} = 3.75$; (c) $N = 382$, $f = 1/3$, $\epsilon^*_{LJ} = 1.75$.

perpendicular to the surface, $R^2_{g,perp}$, defined as

$$R^2_{g,perp} = \frac{1}{N}\langle \sum_{i=1}^{N} (z_i - z_{cm})^2 \rangle \tag{9}$$

where z_i is the Cartesian coordinates of the monomer i in the direction perpendicular to the surface, and the subscript cm stands for the center of mass of the polyion chain, and the molecular axis orientational correlation function, G_2, is defined as

$$G_2 = (3\langle \cos^2 \gamma \rangle - 1)/2 \tag{10}$$

where γ is the angle between the molecular axis and the surface. The molecular axis is defined[43] as the eigenvector corresponding to the smallest eigenvalue of the moment of inertia tensor of the molecule. If the molecular axis aligns parallel to the surface, then $G_2 = -0.5$; if it is perpendicular to the surface, then $G_2 = 1.0$; and if the orientation is isotropic, then $G_2 = 0$.

For a given solvent quality, increasing the surface charge density causes the chain to adsorb flat on the charged surface, and this is manifested in a decrease in G_2. Figure 6a compares G_2 in the ILJ and SASA models, and Figure 6b depicts G_2 in the explicit solvent model as a function of the surface charge density σ^*_{SCD} ($= \sigma_{SCD}\sigma^2/e$) for good and poor solvents, for $N = 16$. For the good solvents, i.e., $\epsilon^*_{LJ} = 0$ or $g^* = 0$, the ILJ and SASA models are identical, and these results are represented by squares. For low surface charge densities the chains are isotropic, but G_2 decreases as σ^*_{SCD} is increased and for $\sigma^*_{SCD} \approx 0.1$ $G_2 \approx -0.5$, corresponding to the chains adsorbed flat on the surface. Similar behavior is also observed in $R^2_{g,perp}$ (not shown). The difference between the models is evident in poor solvents where the SASA predicts that the chains are adsorbed flat on the surface for *all* values of σ^*_{SCD}, whereas the ILJ

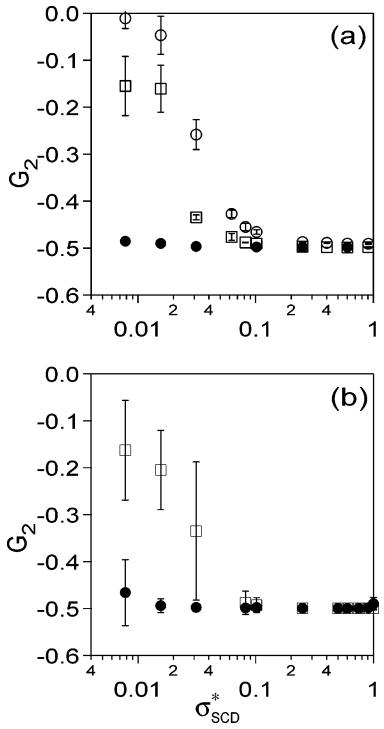

Figure 6. Orientational correlation function G_2 from (a) the ILJ and SASA models and (b) the explicit solvent model, as a function of surface charge density, σ^*_{SCD}, for good and poor solvents. In (a) the symbols represent good solvent (□), i.e., $\epsilon^*_{LJ} = 0$ or $g^* = 0$, and poor solvent, $\epsilon^*_{LJ} = 2$ for the ILJ (○) and $g^* = 1.5$ for the SASA (●). In (b) the symbols represent good solvent (□), $\lambda = 0$ and poor solvent (●), $\lambda = 0.3$.

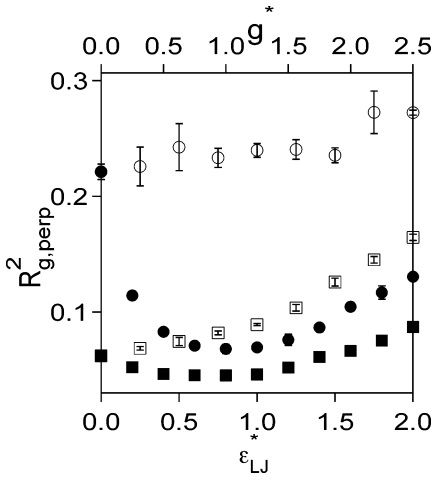

Figure 7. SASA and ILJ model predictions for the average mean-square radius of gyration perpendicular to the surface, as a function of solvent quality for $\sigma^*_{SCD} = 0.1$ (circles) and 0.6 (squares). Solid and open symbols represent SASA and ILJ models, respectively, with the scale represented at the bottom and top of the figure, respectively.

predicts behavior that is qualitatively similar to the good solvent case. The ILJ significantly overestimates the stability of the globular form of the polymer, thus making a flattening against the surface less favorable. The predictions of the SASA model are in quantitative agreement with the explicit solvent simulations (Figure 6b).

Figure 7 depicts $R^2_{g,perp}$ as a function of λ for $\sigma^*_{SCD} = 0.1$ and 0.6. For $\sigma^*_{SCD} = 0.1$ and 0.6, $R^2_{g,perp}$ is a nonmonotonic function of σ^*_{SCD} in the SASA model. The decrease in $R^2_{g,perp}$ occurs because the polyion collapses onto the surface to avoid the unfavorable monomer−solvent interactions. As λ or g^* is increased further, however, the attraction between the monomers overcomes the attraction between the surface and the monomers, and this causes the polyion to form a globule in solution instead of a pancake at the surface. For high surface charge densities, $\sigma^*_{SCD} = 0.6$, the plot, although nonmonotonic, is becoming flat because the monomer−surface interactions are very strong, making it difficult for the polyion to form a globule. These predictions are consistent with the explicit solvent model.[42] In the ILJ model, on the other hand, the solvent-mediated attraction between the surface and the polyion is absent, and the polyion does not collapse onto the surface as you decrease the solvent quality. As a result, $R^2_{g,perp}$ increases monotonically as solvent quality is decreased.

IV. Conclusions

In computer simulations of polymers in poor solvents, simulating the solvent explicitly is prohibitively expensive for the length scales and time scales of interest. In this work, we compare two implicit solvent models, an implicit Lennard-Jones (ILJ), where the solvent effect is incorporated using a LJ potential among the polymer beads, and a solvent-accessible surface area (SASA) model, where the solvent-induced potential depends on the surface area of the polymer molecule, to simulations that incorporate explicit solvent. We investigate three test problems: the collapse dynamics of a neutral polymer, the equilibrium shape of a charged polymer, and the adsorption of a charged polymer to a surface. In most cases, the SASA model is in qualitative agreement with explicit solvent simulations while being much less computationally intensive. The predictions of the ILJ model, on the other hand, are qualitatively different from explicit solvent or SASA models. In many cases, the differences are dramatic. For example, the explicit solvent and SASA models predict a smooth collapse of a polymer for deeper quench depths, whereas the ILJ model predicts the chain gets stuck in metastable states. The explicit solvent and SASA models also predict an adsorption of the chain to a weakly charged surface, whereas the ILJ model predicts that it remains a globule in solution.

For short chains, the predictions of the SASA model for the conformations of charged polymers are consistent with explicit solvent simulations. For long chains, however, the SASA model does not predict the pearl-necklace structures predicted by theory and seen in ILJ model simulations.

We conclude that incorporating the many-body solvent effects is important. The implicit LJ model, which has so far been the model of choice in polymer physics, should be used with caution especially in studying problems where interfaces like surfaces are involved. The implicit solvent model based on the solvent-accessible surface area is a promising candidate as a substitute for explicit solvent. The only concern is that, for the equilibrium size of a single polyelectrolyte chain, it appears that the surface tension parameter in the SASA model must be chain length dependent for the collapse behavior to be consistent with those of the explicit solvent model. It is possible that the model requires a volume term in the interaction,[44] in addition to a SASA term, to properly account for the solution thermodynamics. A resolution of this issue should make the SASA implicit solvent model an exciting alternative to explicit solvent simulations for polyelectrolytes in addition to neutral polymers.

Acknowledgment. This material is based upon work supported by the National Science Foundation under Grant CHE-0315219. G.R. and A.Y. thank Xiao Zhu, Abhishek K. Jha, Professor Rakwoo Chang, and Professor Karl F. Freed for useful

discussions. The graphics in Figures 4 and 5 were made using Visual Molecular Dynamics (VMD).[45]

References and Notes

(1) Baschnagel, J.; Varnik, F. *J. Phys.: Condens. Matter* **2005**, *17*, R851.
(2) Binder, K.; Muller, M.; Virnau, P. *Adv. Polym. Sci.* **2005**, *173*, 1.
(3) Svaneborg, C.; Pedersen, J. *Curr. Opin. Colloid Interface Sci.* **2005**, *173*, 1.
(4) Binder, K.; Baschnagel, J.; Paul, W. *Prog. Polym. Sci.* **2003**, *28*, 115.
(5) Glotzer, S.; Paul, W. *Annu. Rev. Mater. Res.* **2003**, *28*, 115.
(6) Escobedo, F.; de Pablo, J. *Phys. Rep.* **1999**, *318*, 86.
(7) Binder, K.; Milchev, A.; Baschnagel, J. *Annu. Rev. Mater. Res.* **1996**, *26*, 107.
(8) Schueler-Furman, O.; Wang, C.; Bradley, P.; Misura, K.; Baker, D. *Science* **2005**, *310*, 638.
(9) Gumbart, J.; Wang, Y.; Aksimentiev, A.; Tajkhorshid, E.; Schulten, K. *Curr. Opin. Struct. Biol.* **2005**, *15*, 423.
(10) Snow, C.; Sorin, E.; Rhee, Y.; Pande, V. *Annu. Rev. Biophys. Biomol. Struct.* **2005**, *34*, 43.
(11) Micka, U.; Holm, C.; Kremer, K. *Langmuir* **1999**, *15*, 4033.
(12) Chang, R.; Yethiraj, A. *J. Chem. Phys.* **2001**, *114*, 7688.
(13) Chang, R.; Yethiraj, A. *J. Chem. Phys.* **2003**, *118*, 6634.
(14) Feig, M.; Brooks, C., III *Curr. Opin. Struct. Biol.* **2004**, *14*, 217.
(15) Chang, R.; Yethiraj, A. *Macromolecules* **2006**, *39*, 821.
(16) Wodak, S.; Janin, J. *Proc. Natl. Acad. Sci. U.S.A.* **1980**, *77*, 1736.
(17) Grest, G.; Kremer, K. *Phys. Rev. A* **1986**, *33*, 3628.
(18) Bitsanis, I.; Hadziioannou, G. *J. Chem. Phys.* **1990**, *92*, 3827.
(19) Weeks, J. D.; Chandler, D.; Andersen, H. C. *J. Chem. Phys.* **1971**, *54*, 5237.
(20) Tuckerman, M.; Berne, B. J.; Martyna, G. J. *J. Chem. Phys.* **1992**, *97*, 1990.
(21) Nose, S. *J. Chem. Phys.* **1984**, *81*, 511.
(22) Hoover, W. G. *Phys. Rev. A* **1985**, *31*, 1695.
(23) Ermak, D.; McCammon, J. *J. Chem. Phys.* **1978**, *69*, 1352.
(24) Green, D.; Byrne, P.; Dawson, K. *J. Chem. Phys.* **1995**, *102*, 573.
(25) Timoshenko, E.; Kuznetsov, Y. A.; Dawson, K. *J. Chem. Phys.* **1995**, *103*, 4807.
(26) Tanaka, G.; Mattice, W. *Macromolecules* **1995**, *28*, 1049.
(27) Ostrovsky, B.; Bar-Yam, Y. *Europhys. Lett.* **1994**, *25*, 409.
(28) Ostrovsky, B.; Bar-Yam, Y. *Biophys. J.* **1995**, *68*, 1694.
(29) Ostrovsky, B.; Crooks, G.; Bar-Yam, Y. *Phys. Rev. E* **1999**, *60*, 4559.
(30) Straub, J.; Ma, J.; Shakhnovich, J. *J. Chem. Phys.* **1995**, *103*, 2615.
(31) Chan, H.; Dill, K. *J. Chem. Phys.* **1993**, *99*, 2116.
(32) Polson, J. M.; Zuckerman, M. J. *J. Chem. Phys.* **2002**, *116*, 7244.
(33) Abrams, C.; Lee, N.; Obukhov, S. *Europhys. Lett.* **2002**, *59*, 391.
(34) Frisch, T.; Verga, A. *Phys. Rev. E* **2002**, *66*, 041807.
(35) Kikuchi, N.; Gent, A.; Yeomans, J. *Eur. Phys. J. E* **2002**, *9*, 63.
(36) Kikuchi, N.; Ryder, J.; Pooley, C.; Yeomans, J. *Phys. Rev. E* **2005**, *71*, 061804.
(37) Dobrynin, A.; Rubinstein, M. *Macromolecules* **1996**, *29*, 2974.
(38) Lyulin, A.; Dunweg, B.; Borisov, O.; Darinskii, A. *Macromolecules* **1999**, *32*, 3264.
(39) Chodanowski, P.; Stoll, S. *J. Chem. Phys.* **1999**, *111*, 6069.
(40) Micka, U.; Holm, C.; Kremer, K. *Langmuir* **1999**, *15*, 4033.
(41) Micka, U.; Kremer, K. *Europhys. Lett.* **2000**, *49*, 189.
(42) Reddy, G.; Chang, R.; Yethiraj, A. *J. Chem. Theory Comput.* **2006**, *2*, 630.
(43) Yethiraj, A. *Adv. Chem. Phys.* **2002**, *121*, 89.
(44) Wagoner, J. A.; Baker, N. A. *Proc. Natl. Acad. Sci. U.S.A.* **2006**, *103*, 8331−8336.
(45) Humphrey, W.; Dalke, A.; Schulten, K. J. *Mol. Graphics* **1996**, *14*, 33.

MA061176+